Imidazopyridazine inhibitors of *Plasmodium falciparum* calcium dependent protein kinase 1 also target cGMP-dependent protein kinase and heat shock protein 90 to kill the parasite at different stages of intracellular development.

Judith L. Green[a#], Robert W. Moon[a], David Whalley[b], Paul W. Bowyer[c], Claire Wallace[b], Ankit Rochani[d], Rishi Kumar[d], Steven A. Howell[a], Munira Grainger[a], Hayley M. Jones[b], Keith H. Ansell[b], Timothy M. Chapman[b], Debra L. Taylor[b], Simon A. Osborne[b], David A. Baker[c], Utpal Tatu[d], Anthony A. Holder[a#]

The Francis Crick Institute, Mill Hill Laboratory, London, UK[a]; Centre for Therapeutics Discovery, MRC Technology, London, UK[b]; Faculty of Infectious and Tropical Diseases, London School of Hygiene and Tropical Medicine, London, UK[c]; Department of Biochemistry, Indian Institute of Science, Bangalore, India[d]

running title: Imidazopyridazines target *P. falciparum* PKG and HSP90

Address correspondence to judith.green@crick.ac.uk or tony.holder@crick.ac.uk

Abstract

Imidazopyridazine compounds are potent, ATP-competitive inhibitors of calcium dependent protein kinase 1 (CDPK1) and of *Plasmodium falciparum* parasite growth in vitro. Here we show that these compounds can be divided into two classes depending on the nature of the aromatic linker between the core and the R2 substituent group. Class 1 compounds have a pyrimidine linker and inhibit parasite growth at late schizogony whereas class 2 compounds have a non-pyrimidine linker and inhibit growth in the trophozoite stage, indicating different modes of action for the two classes. The compounds also inhibited cGMP-dependent protein kinase (PKG) and their potency against this enzyme was greatly reduced by substitution of the enzyme's gatekeeper residue at the ATP binding site. The effectiveness of the class 1 compounds against a parasite line expressing the modified PKG was also substantially reduced, suggesting that these compounds kill the parasite primarily through inhibition of PKG, rather than CDPK1. HSP90 was identified as a binding partner of class 2 compounds, and a representative compound bound to the ATP-binding site in the N-terminal domain of HSP90. Reducing the size of the gatekeeper residue of CDPK1 enabled inhibition of the enzyme by bumped kinase inhibitors, however a parasite line expressing the modified enzyme showed no change in sensitivity to these compounds. Taken together, these findings suggest that CDPK1 may not be a suitable target for further inhibitor development and that the primary mechanisms through which the imidazopyridazines kill parasites are by inhibition of PKG or HSP90.

Introduction

There is a great need to identify novel targets for anti-malarial therapeutic intervention (1) since the eventual selection of resistance to drug treatments has repeatedly been a problem in the treatment of malaria (2). This is exemplified by the emergence of *Plasmodium falciparum* strains displaying delayed

clearance by the current treatment of choice, artemisinin and its derivatives, and it is considered inevitable that artemisinin resistance will eventually develop and spread (3-5). Recently mutations in the kelch propeller domain protein, K13-propeller, have been shown to be associated with artemisinin resistance in vitro and in vivo (6). New drugs, acting on novel targets, are clearly needed in the ongoing fight against malaria. It is for these reasons that *Plasmodium* protein kinases are now being considered as potential drug targets (7, 8).

Calcium-dependent protein kinase 1 (CDPK1) is an abundant protein expressed in many stages of the *Plasmodium* life cycle. It is indispensable for the development of sexual stages of *P. berghei*, playing a role in activating translation of repressed mRNAs (9). In the asexual blood stages the protein is found at the periphery of merozoites, and is associated with the parasite plasma membrane by virtue of myristoylation and palmitoylation of its N-terminus (10, 11). Its function in blood stages is elusive, with suggestions that it may play a role in regulating parasite motility. The location of the protein on the inner face of the plasma membrane makes it ideally placed to phosphorylate components of the parasite's motor complex that is anchored to both the parasite plasma membrane (PPM) and the inner membrane complex (IMC). Whilst it has been demonstrated that CDPK1 can phosphorylate the myosin light chain MTIP and the glideosome associated protein GAP45 in vitro (10), and that these proteins are modified accordingly in the parasite (12-14), there is no direct evidence that CDPK1 is responsible in vivo. An early study in *P. falciparum* suggested that whilst the *cdpk1* gene was amenable to genetic manipulation, it was not possible to knock it out (15). This suggested an essential role for the protein in blood stages. Initial attempts to delete *cdpk1* in *P. berghei* also proved unsuccessful (16), however in a more recent study the gene was successfully deleted (17).

Apicomplexan CDPKs have been the subject of several drug development programs; these have been summarised in a recent review article (18). There has been a number of studies describing the

development of small molecule inhibitors of CDPK1. For example, the 2,6,9-trisubstituted purine purfalcamine, which blocks *P. falciparum* growth, has been shown by affinity purification to bind to CDPK1 (15). Parasites treated with purfalcamine do not progress through asexual blood stage development, arresting when they are very mature schizonts. This inhibition of merozoite egress suggested a possible role for CDPK1 in this process (15). In a second study, two series of small molecule inhibitors that were competitive for ATP binding to CDPK1 were described (19). We have previously described a series of imidazopyridazine compounds that are potent inhibitors of CDPK1 in vitro, with IC_{50}s in the sub-nanomolar range (20-23). These inhibitors are ATP-competitive; their binding to the recombinant kinase was reduced by a large amino acid at the gatekeeper position and at high concentrations of ATP. Although the most potent of the compounds exhibited an EC_{50} of 12 nM for killing *P. falciparum* in culture, the compounds performed disappointingly in a rodent model of malaria infection. In addition, one puzzling feature of these inhibitors was the poor correlation between their ability to inhibit the enzyme and their ability to block parasite growth, which was suggestive of off-target activity contributing to their inhibitory effects (23).

Here we examine the mechanism of action of some of the inhibitors described previously, and show that they fall into two classes, causing parasite death at two distinct points of the asexual blood stage cycle. We have identified the likely additional target proteins of each class of compound and have been able to identify features of the compounds that confer this selectivity. Furthermore, using a chemical genetics approach, we show that inhibition of CDPK1 does not appear to affect blood stage parasite growth or survival, leading us to conclude that CDPK1 may not be a suitable target for pharmaceutical intervention for the treatment of blood stage malaria infection.

Materials and Methods

Parasite lines and culture methods

All *P. falciparum* lines were maintained in human erythrocytes provided by the National Blood Transfusion Service. 3D7 is a cloned line obtained from the University of Edinburgh. 3D7 PKG T618Q has been described previously (24). Parasites were grown at 2 % hematocrit in RPMI 1640 medium supplemented with 1 % Albumax according to published methods (25). Synchronisation was achieved by centrifugation through a Percoll gradient (26).

Drug treatment and SYBR Green assay

Aliquots of 100 µl *P. falciparum* cultures 24 hours after erythrocyte invasion were transferred into 96-well culture dishes. Cells were incubated with inhibitors for 48 or 96 hours (starting parasitemias were 0.3 % and 0.03 % respectively). All drug treatments were carried out in duplicate at a final dimethyl sulfoxide (DMSO) concentration of 0.05 %. After incubation, a modification of the previously described SYBRGreen assay was performed (27). Cells were lysed by the addition of 25 µl buffer (20 mM Tris-HCl pH 8.0, 2 mM EDTA pH 8.0, 1.6 % Triton X100, 0.16 % saponin, 10x SYBR Green I (Life Technologies). After incubation in the dark for 2 h, fluorescence of the samples was determined using a FLUOStar Omega plate reader (BMG Labtech) with excitation and emission filters of 485 nm and 520 nm respectively. EC_{50} values were calculated from a 4-parameter logistical fit of the data using Prism software (GraphPad Software Inc.). 1-(1, 1-dimethylethyl)-3-(1-naphthalenyl)-1H-pyrazolo[3, 4-d]pyrimidin-4-amine (NA-PP1) and 1-(1, 1-dimethylethyl)-3-(1-naphthalenylmethyl)-1H-pyrazolo[3, 4-d]pyrimidin-4-amine (NM-PP1) were obtained from Merck.

Generation and screening of parasites expressing gatekeeper mutant CDPK1

Parasites expressing CDPK1 T145G and CDPK1 T145T were generated as described previously (28). Briefly, a region of homology to facilitate integration of the plasmid via single crossover homologous recombination was amplified from *P. falciparum* 3D7 genomic DNA: 194 bp upstream of the ATG to base pair 435 of the open reading frame using primers 1 and 2 for the wild-type version and primers 1 and 3 for the glycine version. Each of these fragments was cloned via XmaI and EcoRI sites into a Geneart vector containing a recodonised gene fragment from 436–1572 of the *pfcdpk1* open reading frame. Together, the native and recodonised *cdpk1* sequences were cloned between XmaI and AvrII sites of the pHH4-HA plasmid (29), which adds a triple HA tag at the 3' end followed by a stop codon and the PbDT3' and hDHFR drug selection cassette.

Primer 1: acacCCCGGGGTATACAACGTATAAGACAAATTACTTTTCTTTC

Primer 2: ATATGAATTCGGTTACTAAATAAAAATATTTCTTATCTTCAAAAACATCAAAC

Primer 3: atatGAATTCGCCTACTAAATAAAAATATTTCTTATCTTCAAAAACATCAAAC

P. falciparum 3D7 parasites were transfected with pHH4-CDPK1-HA plasmids (T145T or T145G) using standard methods (30, 31). They were maintained under drug pressure (25 nM WR99210) until resistant parasites emerged, cycled on/off drug, and cloned by limiting dilution.

Clones were screened by PCR using primers 4 and 5 to detect the intact locus and primers 4 and 6 to confirm integration, as well as by Western blot and immunofluorescence using anti-CDPK1 and anti-HA antibodies.

Primer 4: GATGGTGGCACTTGCCTTTTTGAGG

Primer 5: CTGGTTTAATATCTCGATGTACAATATTATGTTTATG

Primer 6: CCCAATCTGTCCCTTAGCTTGTTGTC

Western blotting and immunofluorescence

Late schizont stage parasites were lysed in 1 % NP40, 150 mM NaCl, 10 mM Tris HCl pH 8.0 containing 1 x Complete protease inhibitors (Roche). After centrifugation for 20 min at 15,000 g, 10 µg soluble protein was separated on a 10 % Bis-Tris NuPAGE gel (Life Technologies). Transfer to a nitrocellulose membrane was performed using the iBlot system (Life Technologies). Antibodies against HA (rat monoclonal antibody 3F10; Roche) and CDPK1 (10) were used to detect modified or total CDPK1 respectively, using standard methods.

Recombinant protein production

PfCDPK1 and PfCDPK1 T145G proteins were produced using methods described elsewhere (23). PfHSP90 NTD comprises the first 223 amino acids of PfHSP90. This region was amplified from the full length PfHSP90–pRSET-A construct (32) using primers 7 and 8:

Primer 7: GGCGACGGATCCATGTCAACGGAAACATTCGC

Primer 8: GACCCCCTCGAGCTATTCTTCTTCAGATGCGG

The PCR product was cloned into pRSET-A (Life Technologies) between the BamHI and XhoI sites. Positive clones were confirmed by restriction digestion and sequencing. The clone was transformed into *E. coli* Rosetta pLysS cells and protein was expressed by induction with 0.1 mM isopropyl β-D-1-thiogalactopyranoside (IPTG) at 37 °C for 2 h. PfHSP90 proteins were purified using Ni–NTA affinity chromatography (Qiagen) as described in the manufacturer's protocol.

ParM ADP Biosensor assay

IC_{50} values were determined in kinetic mode using a rhodamine-labelled ParM ADP sensor (Rh-ParM) (33). For these experiments 5 µl of PfCDPK1 (WT or T145G) were diluted in assay buffer (50 mM Tris-HCl pH 8.0, 200 µM $CaCl_2$, 1 mM DTT, 25 mM KCl, 100 µM EGTA and 0.01 % v/v Triton X-

100) to a final concentration of 100 nM and mixed with 10 µl Rh-ParM at a final concentration of 100 nM in black 384-well plates (Corning). Compounds were diluted in half-log series in DMSO and 2 µl volumes of diluted compound, or vehicle to high and low controls, were added to the enzyme and incubated for 30 min at room temperature before initiation of the reaction with 5 µl 20 mM $MgCl_2$ and ATP at the appropriate previously determined K_m value (23): 30 µM and 90 µM ATP for WT CDPK1 and CDPK1 T145G respectively. IC_{50} values were calculated from a 4-parameter logistical fit of the data using Prism software (GraphPad Software Inc.).

Expression and purification of recombinant PKG

Full length PfPKG and PfPKG T618Q were prepared as described previously (24, 34). Briefly, plasmids (pTrcHisC) encoding full length PfPKG and PfPKG T618Q with N-terminal His-tag were transformed into *E. coli* Rosetta2 (DE3). Single colonies were grown in LB Rich Broth (supplemented with 50 µg/ml carbenicillin and 34 µg/ml chloramphenicol) at 37 °C. Protein expression was induced with 1 mM IPTG once an optical density of 0.6–0.7 had been reached. Subsequent overnight growth was at 16 °C. PKGs were purified via the histidine tag on HiTrap TALON columns (GE Healthcare) according to the manufacturer's instructions and then concentrated on 10 kDa molecular weight cut-off concentrators (Amicon). Purified proteins were stored in 50 % glycerol at -80 °C in single use aliquots. Final buffer composition of the purified product was 50 mM Tris HCl pH 7.5, 0.1 mM EGTA, 150 mM NaCl, 0.1 % β-mercaptoethanol, 50 % glycerol, 0.03 % Brij-35, 1 mM benzamidine and 0.2 mM PMSF.

Assay of cGMP-dependent protein kinase activity

IC_{50} values were determined for test compounds using a microfluidic fluorescent shift assay (manuscript in preparation). Briefly, compounds were prepared over a 10-well half-log dilution series in DMSO in duplicate in 50 µl volumes using 96-well polypropylene U-bottomed plates (Thermo Scientific, UK). The reaction mix for each well consisted of 20 µl enzyme/peptide mix (1.25 nM PfPKG or PfPKG T618Q, 1.5 µM FAM-labelled PKAtide [FAM-GRTGRRNSI-NH2, Cambridge Bioscience, UK] in PfPKG assay buffer [25 mM HEPES (pH 7.4), 20 mM β-glycerophosphate, 2 mM DTT, 10 µM cGMP, 0.01 % (w/v) BSA, 0.01 % (v/v) Triton X-100]) plus 5 µl of compound. Samples were pre-incubated at room temperature for 30 min and reactions were initiated by addition of 25 µl ATP mix (10 mM $MgCl_2$ and ATP, at K_m of enzyme under test [20 µM PfPKG and 90 µM PfPKG T618Q], in water). Reactions were terminated at approximately 10 % substrate conversion by addition of 50 µl stop solution (25 mM EDTA in water). Samples were analysed by electrophoretic separation of substrate and product peaks and fluorescence detection using a Caliper Lab Chip EZ reader (Perkin Elmer, Waltham MA) with 0.2 s buffer sip time, downstream voltage 500 V, upstream voltage 1950 V and pressure 0.5 to 1.5 psi. IC_{50} values for the compounds were determined using a 4-parameter logistical fit of the data (GraphPad Prism).

Synthesis of biotinylated compound D

The chemical synthesis of compound D with biotin attached to the R1 or R2 group is described in Supplementary Information 1.

Affinity purification of targets of Compound D

200 µl high capacity streptavidin agarose (Thermo Scientific) was resuspended in 1 ml of 250 µg/ml biotinylated compound D solution, or DMSO control. After incubation with mixing for 1 h at room

temperature unbound compound was removed by extensive washing with PBS. The resin was incubated with trophozoite lysate containing 2 mg protein in a total volume of 1.5 ml overnight at 4 °C. The lysate was prepared by resuspending trophozoites in 20 mM Tris HCl pH 8.0, 10 mM $MgCl_2$, 250 mM NaCl, 0.5 mM tris(2-carboxyethyl)phosphine (TCEP), 1 x protein phosphatase inhibitor (Sigma Aldrich), 1 x complete protease inhibitors (Roche), 0.1 % Triton X-100 (Sigma Aldrich). Insoluble proteins were removed by centrifugation at 15,000 g for 20 min, and protein quantitated using a DC protein assay (Biorad). The resin was extensively washed in lysis buffer to remove unbound proteins, and proteins eluted by resuspending the resin in 100 µl 2 x reducing LDS sample buffer (Life Technologies), with heating at 95 °C for 5 min.

Proteins were run 4 mm into a 10 % NuPAGE Bis Tris gel (Life Technologies), then excised using a clean scalpel blade. Proteins were reduced and alkylated prior to overnight trypsin digestion. The resulting digests were analysed by LC-MS/MS using an Ultimate 3000 nanoRSLC HPLC, equipped with a 50 cm x 75 µm Acclaim Pepmap C18 column, coupled to an LTQ Orbitrap Velos Pro equipped with a Nanoflex electrospray source (all Thermo Scientific). A gradient of 6–32 % acetonitrile/0.1 % formic acid over 48 min was used at a flow rate of 0.3 µl/min. The Orbitrap was operated in Data Dependent Acquisition mode with a survey scan at 60,000 resolution and up to the ten most intense ions selected for MS/MS. Raw files were processed using Proteome Discoverer (PD) 1.3 (Thermo Scientific) with Mascot 2.4 (Matrix Science, UK) as the search engine against the appropriate protein database. A decoy database of reversed sequences was used to filter the results at a false detection rate of 1 %.

K_d Determination for 17-AAG and Compound D binding to PfHSP90

Tryptophan fluorescence analysis was performed using a PerkinElmer LS55 Luminescence spectrometer. In order to determine the binding affinity purified recombinant proteins, 25 µg/ml PfHSP90 or PfHSP90 N-terminal domain (PfHSP90-NTD) were incubated with concentrations of 17-*N*-allylamino-17-demethoxygeldanamycin (17-AAG) or Compound D ranging from 0-60 µM. The binding buffer used for the reaction contained 50 mM Tris-HCl pH 7.4 and 1 mM EDTA. Samples were excited at 280 nm and tryptophan fluorescence measurements were carried out by scanning the emission spectrum in the wavelength range 300-400 nm. λ_{max} of 346 nm was selected for all the calculations. The slit-width of excitation and emission was set at 2.5 and 5 nm respectively. The difference in fluorescence intensity of protein alone compared with various concentrations of 17-AAG or compound D was calculated and plotted against the different concentrations of the respective ligand used. The resultant hyperbolic curve was analysed with GraphPad Prism software, using non-linear regression analysis with single site-specific binding as described previously (32).

Docking compound D to PfHSP90

Docking calculations were performed using the web based graphical user interface (GUI) of Docking Server (www.dockingserver.com) by Virtua Drug (35). PfHSP90 N-terminal domain structure was downloaded from PDB (PDB: 3k60) (36). Chain A of the dimeric PfHSP90 was used to perform docking calculations. Essential hydrogen atoms, Kollman united atom type charges, and solvation parameters were added with the aid of AutoDock tools (37). An affinity map of 20x20x20 Å grid points and 0.375 Å spacing was developed using the Autogrid program (37). Test and control ligand structures were subjected to geometry optimization and charge calculations were performed using MMFF94 and Gasteiger methods respectively (38). Here, Gasteiger partial charges were added to the ligand atoms. Non-polar hydrogen atoms were merged, and rotatable bonds were defined. AutoDock parameter set

and distance-dependent dielectric functions were used in the calculation of the Van der Waals and the electrostatic terms respectively.

The prepared molecular structures were subjected to docking simulation using the Lamarckian genetic algorithm (LGA) and the Solis and Wets local search method (39) which is used by the Docking Server GUI. All rotatable torsions were released during docking. During the search, a translational step of 0.2 Å and torsional steps of 5.0 Å were applied. Docking calculations are the result of ten autonomous runs. Each run was terminated after a maximum of 250,000 energy evaluations. The population size was set to 150. Here, we used free energy of binding (kcal/mol), number of hydrogen bond interactions, inhibition constant *Ki* and frequency of probable binding sites for ranking our docking results. Frequency shows the percentage of the local searches with similar geometry having root mean square tolerance (rmstol) of 2 Å. Docked structures with the lowest free energy of binding and K_i values, structures having two or more hydrogen bond interactions between ligand and protein and the frequency of 10 % or more were used for prediction of the probable binding configuration for Compound D. The analysed .pdb format of the docking file was downloaded and analysed using Discovery Studio Visualizer 4.0.

Results

Imidazopyridazines target two distinct stages of asexual parasite development

Previously we developed a series of potent CDPK1 inhibitors based on an invariant imidazopyridazine central core, an aromatic linker group (A), and variable R1 and R2 groups (Figure 1A). Some of these compounds inhibit recombinant CDPK1 with low nanomolar IC_{50}s, and are extremely effective at killing parasites in culture, with the most potent compound having an EC_{50} of 12 nM (20-23). To determine their mode of action against the parasite we added the compounds to synchronised parasite

populations and identified at which stage they inhibited growth. Examination of Giemsa-stained smears of parasites treated at the ring stage with imidazopyridazines at ten times their parasiticidal EC_{50} revealed that the compounds had two distinct mechanisms of action during intracellular development. Some (designated class 1 compounds) killed parasites at the mature schizont stage late in the cycle, whilst others (class 2 compounds) killed parasites at the early trophozoite stage (Figure 1B). In the former case, whilst parasites developed into schizonts in the presence of the compounds, they did not rupture the erythrocyte to release merozoites.

As a higher throughput alternative to microscopic examination, we used a fluorescence-based assay to measure parasite DNA content. Briefly, a trophozoite population collected 21 hours after merozoite invasion of erythrocytes was incubated with compound for either 48 or 96 hours: one or two rounds of parasite replication. Parasites were then lysed in the presence of SYBR Green I, a fluorescent dye that binds preferentially to double-stranded DNA. After 48 hours incubation, parasites treated with compounds that kill following DNA replication will be indistinguishable from untreated cells, because an arrested schizont will give the same net fluorescence as parasites from a ruptured schizont that have gone on to invade red blood cells. Extending the culture period after drug addition to 96 hours enables a true EC_{50} to be measured for all compounds, because another round of parasite replication will have occurred in viable parasites. The EC_{50} measured for compounds that act prior to DNA synthesis will be identical regardless of the incubation time, whereas compounds that act after DNA synthesis will appear to be much less potent in the shorter incubation assay. Use of these two measures enabled compounds to be classified based on the stage at which they killed parasites. Class 1 compounds act after DNA synthesis in late schizogony and prior to merozoite release, whereas class 2 compounds act at the trophozoite stage prior to DNA synthesis. Graphs for exemplar compounds of each class are shown in Figure 1C.

We analysed 41 compounds in this manner in order to define the molecular features that determine their mode of action (Table S1). For each compound the EC_{50} value was measured at 48 hours ($EC_{50}48$) and 96 hours ($EC_{50}96$) and the ratio of the EC_{50}s was calculated; an $EC_{50}48/EC_{50}96$ ratio greater than five was a strong indication that a compound acted after DNA synthesis. When the structure of each compound was examined, a determinant of the stage at which the compounds acted was the presence or absence of a pyrimidine at the aromatic linker position (labelled A in Figure 1A). Of the 16 compounds with a pyrimidine linker, 13 had an $EC_{50}48$:$EC_{50}96$ ratio greater than 5, suggesting that their action was after DNA synthesis (class 1). Of the 25 compounds with non-pyrimidine linkers, 24 had an $EC_{50}48$:$EC_{50}96$ ratio less than 5, suggesting their action was prior to DNA synthesis (class 2). Full details are provided in Table S1. This classification was again confirmed by microscopic examination of Giemsa stained blood smears of parasites treated with a subset of ten compounds (Tables 1 and S1). Compound 28 was the only class 1 compound in Table 1 with an $EC_{50}48$:$EC_{50}96$ ratio less than 5, and was confirmed by microscopy to arrest parasites in late schizogony, indicating that whilst an $EC_{50}48$:$EC_{50}96$ ratio greater than 5 is suggestive of action after DNA replication, borderline cases need to be confirmed by microscopy. The majority of class 1 compounds (9 of 16) have an $EC_{50}48$:$EC_{50}96$ ratio greater than 500.

Late acting compounds kill parasites by inhibiting cGMP-dependent kinase (PKG)

We first wished to identify the target of the class 1 inhibitors in the parasite since, although they act very late in schizogony, they may be acting through a target other than CDPK1. For example, the phenotype of parasites treated with purfalcamine, a previously reported CDPK1 inhibitor (15), is very reminiscent of those treated with cGMP-dependent protein kinase (PKG) inhibitors such as ‘compound 1’, in which merozoites develop within the schizont but are not released because of a defect in egress

(40). Whilst it is not impossible that the phenotype of CDPK1 inhibition is indistinguishable from that of PKG inhibition, we wished to definitively identify the primary target(s) of our compounds. CDPK1 and PKG are closely related kinases with regard to the ATP binding site, for example they share some sequence homology including a small threonine residue at the gatekeeper position (residue 145 in CDPK1 and 618 in PKG). The imidazopyridazine compounds in this study have been shown to interact at the ATP binding site of recombinant CDPK1 in vitro and this binding was blocked by substitution of the gatekeeper residue with the larger glutamine, which blocks access to the enzyme's binding pocket rendering it relatively insensitive to specific inhibitors (23). In a similar chemical genetics approach the gatekeeper residue of PKG had also been substituted by glutamine (24).

We tested the ability of 30 compounds to inhibit PKG, and their sensitivity to a large residue at the gatekeeper position. All of the compounds inhibited recombinant PKG activity, with the most potent compound having an IC_{50} of 1.55 nM (Table S2). We have shown previously that the correlation of IC_{50} for CDPK1 and *P. falciparum* EC_{50} for these compounds was poor (23). When compounds were grouped according to class 1 and 2, there was an excellent correlation between PKG IC_{50} and parasite-killing EC_{50} where the aromatic linker is a pyrimidine (class 1), (Figure 2Ai). Where the linker group is not a pyrimidine (class 2) the correlation was poor (Figure 2Aii). All of the compounds tested against PKG relied on the presence of a small gatekeeper residue for their activity. Substitution of threonine 618 with glutamine resulted in an increase in IC_{50} value by a factor of between 20 and over 16000 (Tables 2 and S2).

To establish whether PKG was the primary target of the inhibitors in the parasite, we used a parasite line expressing a variant PKG T618Q enzyme (24) and measured the EC_{50} of six class 1 and five class 2 compounds against 3D7 wild-type (WT) and PKG T618Q parasites, using the SYBR Green I assay described previously, with a 96 h incubation time. We also included 'compound 1', a tri-substituted

pyrrole previously shown to be an apicomplexan PKG inhibitor that is also sensitive to the size of the gatekeeper residue (24). All but one of the class 1 compounds had a decreased parasiticidal activity against the PKG T618Q variant parasite, with compound B (a class 1 compound) showing the greatest effect: a 29-fold decrease in potency (Table 2 and Figure 2B). The exception is compound 44, a class 1 compound with an isobutyl aliphatic group at position R2, whereas the others have fluorophenyl R2 groups. It is possible that the smaller aliphatic R2 group enables this compound to bind to the modified enzyme, despite the large gatekeeper residue. Examination of Giemsa-stained smears of 3D7 parasites treated at the ring stage with compound 44 at its EC_{90} (0.65 µM) showed that the parasites were arrested at the schizont stage, suggesting that it behaves like other class 1 compounds in terms of its mode of parasite killing. 'Compound 1' showed a seven-fold decrease in potency against the PKG T618Q parasite, in line with previously published data (24, 40). In contrast, none of the class 2 compounds (non-pyrimidine linker group) showed a significant increase in EC_{50} against the PKG T618Q parasite, (Tables 2 and S2). To determine the statistical significance of the difference between the two classes of compounds, a Mann-Whitney test was performed. The median ratio EC_{50} 3D7 PKG T618Q:EC_{50} 3D7 for class 1 compounds was 16.8 and for class 2 compounds the median EC_{50} ratio was 1.4. The p value was calculated to be 0.0043, indicating that the difference between these two classes of compounds is significant (Figure 2C). Taken together, these data strongly suggest that the class 1 compounds exert their parasiticidal effect primarily through inhibition of PKG activity, whereas the class 2 compounds do not.

Early acting compounds may kill parasites by inhibiting HSP90

The early stage of the asexual cycle targeted by class 2 compounds precludes the target from being CDPK1 as it is not expressed in such early parasites (41-43). To identify their target, we selected an

exemplar class 2 compound, compound D, resynthesized it with biotin attached to the R1 group (Figure 3A), and made an affinity resin using streptavidin agarose. We purified interacting proteins from a lysate prepared from infected erythrocytes approximately 24 hours after invasion by merozoites, and identified interacting proteins by LC-MS/MS. For proteins to be defined as hits they had to be present in replicate LC-MS/MS analyses with compound D resin, and absent from duplicate control resin assays, one with unloaded streptavidin and another where the biotin was attached to the R2 group. Most of the proteins detected were very weak hits, with fewer than five unique peptides identified. The only exception was HSP90 (PF3D7_0708400), which had 24 unique peptide hits (Table S3). HSP90 is a protein chaperone with an ATP binding site in its N-terminal domain. Using in silico methods we judged that the free energy of binding of compound D to the ATP-binding pocket of PfHSP90 was favourable; Figure 3B shows the residues of PfHSP90 predicted to interact with compound D, and Figure 3C shows the most likely binding orientation of the compound. From the docking simulation it can be predicted that compound D will form both polar and hydrophobic interactions with the amino acid residues in the binding pocket of PfHsp90. Our analysis suggests that the nitrogen atom of the piperidine group may attain a quaternary state to form a hydrogen bond interaction with the carboxyl group of Asp40. In the given orientation the amino linker between the imidazopyridazine and piperidine groups might also form a hydrogen bond interaction with Asn37. Further, the pyridine (aromatic linker) in compound D could form a mixed pi/ alkyl hydrophobic interaction with Leu93. We found that the amino alkyl branched chain attached to the aromatic linker may also interact with Leu34, Ala38, and Ile173 to promote the formation of a stable protein-ligand complex. In addition, Phe124 may interact with the imidazopyridazine nucleus of compound D by both pi and alkyl hydrophobic interactions. The Gibbs binding free energy for the selected orientation of compound D in the binding pocket of PfHSP90 was found to be -7.42 kcal/mol with root mean square tolerance (rmstol) of 2 Å. It

Antimicrobial Agents and Chemotherapy

is well established that the K_d value of a compound depends on the Gibbs binding free energy (44). The K_i value for the compound was predicted to be 3.64 µM. The interaction of compound D with recombinant PfHSP90 and the N-terminal domain of HSP90 (PfHSP90-NTD) in vitro was confirmed by measuring changes in intrinsic tryptophan fluorescence upon binding (32). The K_d values obtained for compound D binding to full-length PfHSP90 and PfHSP90-NTD were 6.17 and 10.73 µM respectively. In both cases the data indicated a slightly stronger interaction than that of 17-AAG, an established HSP90 inhibitor (45) (Figure 3D).

Inhibition of CDPK1 has no effect on asexual parasite development

To unequivocally determine the effect of inhibiting CDPK1 on asexual blood stage parasite development, we adopted a chemical genetics approach. Modification of the gatekeeper residue of a kinase can alter its sensitivity to a group of large inhibitors known as bumped kinase inhibitors (BKIs). Kinases with large gatekeeper residues tend to be insensitive to these inhibitors, whereas those with small gatekeeper residues are more sensitive (46, 47). The CDPK1 T145G enzyme, which has the smallest amino acid—glycine—at this position, has kinase activity in line with that of the wild-type enzyme, and is sensitive to inhibition by the imidazopyridazine compounds (23). We tested two chemically related BKIs, NA-PP1 and NM-PP1, which are identical excepting the extended methylene linker of NM-PP1, which causes the orientation of the napthyl group to change relative to the pyrazolopyrimidine core (Figure 4A). Both of these compounds are reversible, cell-permeable inhibitors of small gatekeeper residue kinases and have been used in both mammalian (48, 49) and yeast cells (47, 50). CDPK1-T145G was 41 times more sensitive than the wild-type enzyme to inhibition by NA-PP1—IC_{50}s 0.15 and 6.01 µM respectively—and 13 times more sensitive to NM-PP1 than the wild-type enzyme—IC_{50}s 0.12 and 1.50 µM respectively—(Figure 4B). We used statistical

analysis within GraphPad Prism to compare the individual curve fits for each data set with a curve fit to all the data sets, with a null hypothesis that the IC_{50} values are the same for both data sets. An extra-sum-of-squares F test was used to compare the goodness-of-fit of the two alternative models. A p value of <0.0001 indicated that one curve did not fit to both data sets as well as individual curves, and that the IC_{50} values are therefore significantly different for both inhibitors with the two variant enzymes. Having established this differential sensitivity of a gatekeeper variant CDPK1, we generated by homologous recombination at the endogenous gene locus a parasite line that expressed CDPK1-T145G. The transgenic parasite was engineered to also express a triple HA-tag at the extreme C-terminus of the enzyme. A control parasite line was made using an identical targeting approach in which a triple HA-tag was added to the protein but no amino acid substitution was introduced at the gatekeeper residue (Figure 4C). Using an anti-HA antibody on western blots of schizont lysates from the parasite lines, the modified proteins were the expected size and there was no evidence of unmodified protein in either line (Figure 4Di). The T145G variant protein was expressed in late-stage schizonts and targeted to the periphery of merozoites in the same way as the wild-type enzyme (Figure 4Dii). The two parasite lines were incubated with NA-PP1 and NM-PP1 and the EC_{50}s for each compound were calculated (Figure 4E). The EC_{50} for NA-PP1 was 14.26 µM for 3D7 CDPK1-T145T and 15.65 µM for 3D7 CDPK1-T145G. For NM-PP1 the EC_{50}s were 11.55 µM and 10.28 µM for 3D7 CDPK1-T145T and 3D7 CDPK1-T145T parasite lines respectively. An extra-sum-of-squares F test to compare the fit of one curve to both data sets with that of individual curves for each data set, with a null hypothesis that the same curve could fit both data sets, gave a p value of 0.70 for NA-PP1 treatment of the two parasite lines, and 0.79 for NM-PP1, indicating that the same curve could be used to fit the data for both parasite lines with the inhibitors and that there is no significant difference between the sensitivity of the

parasite lines to either of the BKIs. These data suggest that inhibition of CDPK1 has no effect on asexual parasite viability.

Discussion

The need for novel drugs against malaria has resulted in the emergence of protein kinases as potential new targets (7). Whilst little is known about their detailed role in the biology of the parasite, evidence from reverse genetics approaches regarding the essentiality of a kinase has guided target selection (12). One such kinase is PfCDPK1, which had been thought to be essential in asexual blood stages due to an inability to disrupt the gene in *P. falciparum* and *P. berghei* (15, 16).

We have characterised a series of imidazopyridazines that were developed as CDPK1 inhibitors (20-23). We show here that the parasiticidal activity of the compounds falls into two distinct classes based on the timing of action during the asexual cycle of *P. falciparum*. Furthermore, we established that the stage in the asexual cycle at which the compounds act is governed by the nature of the aromatic linker group. Class 1 compounds with a pyrimidine ring at this position killed parasites at late schizogony, by inhibition of PKG. Class 2 compounds with a non-pyrimidine moiety at this position cause parasite death at the trophozoite stage, probably by inhibiting the activity of HSP90. It is remarkable that the mode of action of the inhibitors is changed by relatively small changes in the aromatic linker group.

We have demonstrated that the primary target of Class 1 imidazopyridazines is PKG, and the consequence of this inhibition is a failure of merozoites to egress from schizonts. Although we had shown previously that CDPK1 is potently inhibited by these compounds (23), it appears that inhibition of CDPK1 has no effect on parasite development: when an effect on PKG is discounted by using a parasite expressing an inhibitor-insensitive PKG, the parasite's sensitivity to the compounds is very substantially reduced. If inhibition of CDPK1 contributed to the observed effect on merozoite egress

then we would have expected the PKG T618Q parasite line to retain sensitivity to these compounds, which it did not.

The identification of the protein chaperone HSP90 by affinity purification with compound D was unexpected, as the compounds had been developed as kinase inhibitors. However, HSP90 has essential ATPase activity and it is likely that the class 2 imidazopyridazine compounds bind to the ATP-binding site of both HSP90 and CDPK1, even though these binding sites are quite dissimilar. It is possible that the inhibitory phenotype seen in trophozoites in the presence of class 2 compounds may be caused by the inhibition of kinases or ATPases in addition to HSP90 that were not identified in the affinity purification using compound D. However it remains that HSP90 is a most promising candidate based on the experiments we have presented here. The binding of compound D to HSP90 was confirmed experimentally. The use of HSP90 inhibitors to block malaria parasite development is not a new concept. Geldanamycin is a benzoquinone ansamycin known to be an ATP-competitive inhibitor of human HSP90 (51). Both geldanamycin and its derivative 17-AAG have been shown to block parasite development at the trophozoite stage and to inhibit the ATPase activity of *P. falciparum* HSP90 (32, 52). Another HSP90 inhibitor is the purine analogue, PU-H71, which has anti-parasite activity in vitro and in vivo, and displays a significant synergistic effect with chloroquine (53). A series of 7-azaindole compounds show exquisite binding selectivity for the parasite HSP90 over the human isoforms and have been shown to inhibit *P. falciparum* growth in culture (54). The class 2 imidazopyridazines represent a new starting point to generate *Plasmodium*-specific HSP90 inhibitors.

Using a chemical genetics approach, we produced a *P. falciparum* line that expresses a CDPK1 gatekeeper variant that displays increased sensitivity to bumped kinase inhibitors. There was no difference in the sensitivity to either BKI of this parasite line and one expressing an unchanged CDPK1. This supports the notion that inhibiting CDPK1 may not have an effect on parasite viability,

and that the imidazopyridazine compounds kill parasites by inhibition of other enzymes, despite their extremely potent inhibition of CDPK1 activity in vitro (and presumably in vivo). Both of the BKIs used in this study have been demonstrated to be cell-permeable in several other systems (47-50), so it is reasonable to presume that *P. falciparum* is also accessible to inhibition with these compounds. Similar chemical genetics approaches have been adopted to study the orthologue of CDPK1 in *Toxoplasma gondii,* TgCDPK3. Lourido and colleagues identified subtle differences in gliding motility when parasites expressing TgCDPK3 with a glycine gatekeeper residue were treated with BKIs, and the ability to respond to ionophore-induced increases in intracellular calcium was impaired (55). There are differences in parasite biology and likely mechanisms of egress between *T. gondii* and *P. falciparum* and therefore direct extrapolation of results from either system to the other may be unwise (56).

Our view that CDPK1 may not be essential in *P. falciparum* asexual blood stages is supported by recent studies in *P. berghei.* Sebastian and colleagues showed that when using a promoter-swap approach to express PbCDPK1 at almost undetectable levels in asexual blood stages there was no effect on parasite development during these stages (9). More recently, while our investigations were ongoing, a study that knocked out the *pbcdpk1* gene demonstrated conclusively that PbCDPK1 is entirely dispensable in blood stages, with no effect on any stage of asexual parasite development (17). There is no reason to think that CDPK1 plays different roles in *P. falciparum* and *P. berghei*; indeed *pfcdpk1* can substitute for *pbcdpk1* with no obvious effect on *P. berghei* at any stage of development (Dr. R. Tewari, personal communication).

Purfalcamine, a 2,6,9-trisubstituted purine, has been identified as an inhibitor of PfCDPK1 and in its presence *P. falciparum* parasites accumulate in late schizogony, with a block of merozoite egress (15). Whilst there is no doubt that purfalcamine potently inhibits recombinant CDPK1, it is possible that it exerts its parasiticidal effect by inhibiting enzymes other than CDPK1, such as PKG or perhaps other

CDPKs such as CDPK4 or CDPK5, which is known to be involved in merozoite egress (57). It will be important to establish whether or not the parasiticidal effect of purfalcamine is sensitive to the size of the PKG gatekeeper residue.

Target validation for drug discovery can be a complex process, and extrapolating from genetic knockout studies to the consequences of inhibition by small molecules can be problematic (58). Where the phenotype of a genetic knockout is in doubt, target-based drug discovery can lead to the erroneous attribution of off-target activities of compounds to the protein of interest. The evidence we have presented casts considerable doubt on the suitability of CDPK1 as a drug target for blood-stage *Plasmodium* infections. Whilst it may represent a target for transmission-blocking treatment, owing to its proven role in the sexual stages of the parasite (9), it seems that inhibition of the enzyme during the asexual cycle causes no measurable reduction in fitness of the parasite and as such CDPK1 may not be worth pursuing as a drug target for the asexual stages of *Plasmodium*.

Acknowledgements

This work was supported by the Francis Crick Institute, which receives its core funding from Cancer Research UK, the UK Medical Research Council, and the Wellcome Trust. In addition, this research was supported by the EviMalar Network of Excellence (FP7 grant agreement 242095) to AAH; Medical Research Council UK, Developmental Pathway Funding Scheme Grant (Ref: G10000779) and Wellcome Trust Project Grant (ref: 094752) to DAB.

References

1. **Enserink M**. 2010. As challenges change, so does science. Science **328**:843

2. **Klein EY**. 2013. Antimalarial drug resistance: a review of the biology and strategies to

delay emergence and spread. International Journal of Antimicrobial Agents **41**:311–317.

3. **Dondorp AM**, **Nosten F**, **Yi P**, **Das D**, **Phyo AP**, **Tarning J**, **Lwin KM**, **Ariey F**, **Hanpithakpong W**, **Lee SJ**, **Ringwald P**, **Silamut K**, **Imwong M**, **Chotivanich K**, **Lim P**, **Herdman T**, **An SS**, **Yeung S**, **Singhasivanon P**, **Day NPJ**, **Lindegardh N**, **Socheat D**, **White NJ**. 2009. Artemisinin resistance in *Plasmodium falciparum* malaria. N Engl J Med **361**:455–467.

4. **Ferreira PE**, **Culleton R**, **Gil JP**, **Meshnick SR**. 2013. Artemisinin resistance in *Plasmodium falciparum*: what is it really? Trends Parasitol **29**:318–320.

5. **Noedl H**. 2005. Artemisinin resistance: how can we find it? Trends Parasitol **21**:404–405.

6. **Ariey F**, **Witkowski B**, **Amaratunga C**, **Beghain J**, **Langlois A-C**, **Khim N**, **Kim S**, **Duru V**, **Bouchier C**, **Ma L**, **Lim P**, **Leang R**, **Duong S**, **Sreng S**, **Suon S**, **Chuor CM**, **Bout DM**, **Ménard S**, **Rogers WO**, **Genton B**, **Fandeur T**, **Miotto O**, **Ringwald P**, **Le Bras J**, **Berry A**, **Barale J-C**, **Fairhurst RM**, **Benoit-Vical F**, **Mercereau-Puijalon O**, **Ménard D**. 2014. A molecular marker of artemisinin-resistant *Plasmodium falciparum* malaria. Nature **505**:50–55.

7. **Doerig C**. 2004. Protein kinases as targets for anti-parasitic chemotherapy. Biochim Biophys Acta **1697**:155–168.

8. **Doerig C**, **Billker O**, **Pratt D**, **Endicott J**. 2005. Protein kinases as targets for antimalarial intervention: Kinomics, structure-based design, transmission-blockade, and targeting host cell enzymes. Biochim Biophys Acta **1754**:132–150.

9. **Sebastian S**, **Brochet M**, **Collins MO**, **Schwach F**, **Jones ML**, **Goulding D**, **Rayner JC**, **Choudhary JS**, **Billker O**. 2012. A *Plasmodium* Calcium-Dependent Protein Kinase Controls Zygote Development and Transmission by Translationally Activating Repressed

mRNAs. Cell Host Microbe **12**:9–19.

10. **Green JL**, **Rees-Channer RR**, **Howell SA**, **Martin SR**, **Knuepfer E**, **Taylor HM**, **Grainger M**, **Holder AA**. 2008. The Motor Complex of *Plasmodium falciparum*: phosphorylation by a calcium-dependent protein kinase. J Biol Chem **283**:30980–30989.

11. **Möskes C**, **Burghaus PA**, **Wernli B**, **Sauder U**, **Dürrenberger M**, **Kappes B**. 2004. Export of *Plasmodium falciparum* calcium-dependent protein kinase 1 to the parasitophorous vacuole is dependent on three N-terminal membrane anchor motifs. Mol Microbiol **54**:676–691.

12. **Solyakov L**, **Halbert J**, **Alam MM**, **Semblat J-P**, **Dorin-Semblat D**, **Reininger L**, **Bottrill AR**, **Mistry S**, **Abdi A**, **Fennell C**, **Holland Z**, **Demarta C**, **Bouza Y**, **Sicard A**, **Nivez M-P**, **Eschenlauer S**, **Lama T**, **Thomas DC**, **Sharma P**, **Agarwal S**, **Kern S**, **Pradel G**, **Graciotti M**, **Tobin AB**, **Doerig C**. 2011. Global kinomic and phospho-proteomic analyses of the human malaria parasite *Plasmodium falciparum*. Nat Commun **2**:565–12.

13. **Lasonder E**, **Green JL**, **Camarda G**, **Talabani H**, **Holder AA**, **Langsley G**, **Alano P**. 2012. The *Plasmodium falciparum* Schizont Phosphoproteome Reveals Extensive Phosphatidylinositol and cAMP-Protein Kinase A Signaling. J Proteome Res **11**:5323–5337.

14. **Lasonder E**, **Green JL**, **Grainger M**, **Langsley G**, **Holder AA**. 2015. Extensive differential protein phosphorylation as intraerythrocytic *Plasmodium falciparum* schizonts develop into extracellular invasive merozoites. Proteomics doi: 10.1002/pmic.201400508

15. **Kato N**, **Sakata T**, **Breton G**, **Le Roch KG**, **Nagle A**, **Andersen C**, **Bursulaya B**, **Henson K**, **Johnson J**, **Kumar KA**, **Marr F**, **Mason D**, **McNamara C**, **Plouffe D**,

Ramachandran V, **Spooner M**, **Tuntland T**, **Zhou Y**, **Peters EC**, **Chatterjee A**, **Schultz PG**, **Ward GE**, **Gray N**, **Harper J**, **Winzeler EA**. 2008. Gene expression signatures and small-molecule compounds link a protein kinase to *Plasmodium falciparum* motility. Nat Chem Biol **4**:347–356.

16. **Tewari R**, **Straschil U**, **Bateman A**, **Böhme U**, **Cherevach I**, **Gong P**, **Pain A**, **Billker O**. 2010. The Systematic Functional Analysis of *Plasmodium* Protein Kinases Identifies Essential Regulators of Mosquito Transmission. Cell Host Microbe **8**:377–387.

17. **Jebiwott S**, **Govindaswamy K**, **Mbugua A**, **Bhanot P**. 2013. *Plasmodium berghei* Calcium Dependent Protein Kinase 1 Is Not Required for Host Cell Invasion. PLoS ONE **8**:e79171.

18. **Hui R**, **Bakkouri El M**, **Sibley LD**. 2015. Designing selective inhibitors for calcium-dependent protein kinases in apicomplexans. Trends Pharmacol Sci **36**:452–460.

19. **Lemercier G**, **Fernandez-Montalvan A**, **Shaw JP**, **Kugelstadt D**, **Bomke J**, **Domostoj M**, **Schwarz MK**, **Scheer A**, **Kappes B**, **Leroy D**. 2009. Identification and Characterization of Novel Small Molecules as Potent Inhibitors of the Plasmodial Calcium-Dependent Protein Kinase 1. Biochemistry **48**:6379–6389.

20. **Chapman TM**, **Osborne SA**, **Bouloc N**, **Large JM**, **Wallace C**, **Birchall K**, **Ansell KH**, **Jones HM**, **Taylor D**, **Clough B**, **Green JL**, **Holder AA**. 2013. Substituted imidazopyridazines are potent and selective inhibitors of *Plasmodium falciparum* calcium-dependent protein kinase 1 (PfCDPK1). Bioorg Med Chem Lett **23**:3064–3069.

21. **Large JM**, **Osborne SA**, **Smiljanic-Hurley E**, **Ansell KH**, **Jones HM**, **Taylor DL**, **Clough B**, **Green JL**, **Holder AA**. 2013. Imidazopyridazines as potent inhibitors of *Plasmodium falciparum* calcium-dependent protein kinase 1 (PfCDPK1): Preparation and

evaluation of pyrazole linked analogues. Bioorg Med Chem Lett **23**:6019–6024.

22. **Chapman TM**, **Osborne SA**, **Wallace C**, **Birchall K**, **Bouloc N**, **Jones HM**, **Ansell KH**, **Taylor DL**, **Clough B**, **Green JL**, **Holder AA**. 2014. Optimization of an imidazopyridazine series of inhibitors of *Plasmodium falciparum* calcium-dependent protein kinase 1 (PfCDPK1). J Med Chem **57**:3570–3587.

23. **Ansell KH**, **Jones HM**, **Whalley D**, **Hearn A**, **Taylor DL**, **Patin EC**, **Chapman TM**, **Osborne SA**, **Wallace C**, **Birchall K**, **Large J**, **Bouloc N**, **Smiljanic-Hurley E**, **Clough B**, **Moon RW**, **Green JL**, **Holder AA**. 2014. Biochemical and Antiparasitic Properties of Inhibitors of the *Plasmodium falciparum* Calcium-Dependent Protein Kinase PfCDPK1. Antimicrobial Agents and Chemotherapy **58**:6032–6043.

24. **McRobert L**, **Taylor C**, **Deng W**, **Fivelman Q**, **Cummings R**, **Polley S**, **Billker O**, **Baker D**. 2008. Gametogenesis in Malaria Parasites Is Mediated by the cGMP-Dependent Protein Kinase. PLoS Biol **6**:e139.

25. **Trager W**, **Jensen JB**. 1976. Human malaria parasites in continuous culture. Science **193**:673–675.

26. **Lambros C**, **Vanderberg J**. 1979. Synchronization of *Plasmodium falciparum* erythrocytic stages in culture. J Parasitol **65**:418–420.

27. **Smilkstein M**, **Sriwilaijaroen N**, **Kelly JX**, **Wilairat P**, **Riscoe M**. 2004. Simple and inexpensive fluorescence-based technique for high-throughput antimalarial drug screening. Antimicrobial Agents and Chemotherapy **48**:1803–1806.

28. **Alam MM**, **Solyakov L**, **Bottrill AR**, **Flueck C**, **Siddiqui FA**, **Singh S**, **Mistry S**, **Viskaduraki M**, **Lee K**, **Hopp CS**, **Chitnis CE**, **Doerig C**, **Moon RW**, **Green JL**, **Holder AA**, **Baker DA**, **Tobin AB**. 2015. Phosphoproteomics reveals malaria parasite

Protein Kinase G as a signalling hub regulating egress and invasion. Nat Commun **6**:1–15.

29. **Yusuf NA**, **Green JL**, **Wall RJ**, **Knuepfer E**, **Moon RW**, **Schulte-Huxel C**, **Stanway RR**, **Martin SR**, **Howell SA**, **Douse CH**, **Cota E**, **Tate EW**, **Tewari R**, **Holder AA**. 2015. The *Plasmodium* Class XIV Myosin, MyoB, Has a Distinct Subcellular Location in Invasive and Motile Stages of the Malaria Parasite and an Unusual Light Chain. J Biol Chem **290**:12147–12164.

30. **Wu Y**, **Sifri CD**, **Lei HH**, **Su XZ**, **Wellems TE**. 1995. Transfection of *Plasmodium falciparum* within human red blood cells. Proc Natl Acad Sci USA **92**:973–977.

31. **Fidock DA**, **Wellems TE**. 1997. Transformation with human dihydrofolate reductase renders malaria parasites insensitive to WR99210 but does not affect the intrinsic activity of proguanil. Proc Natl Acad Sci USA **94**:10931–10936.

32. **Pallavi R**, **Roy N**, **Nageshan RK**, **Talukdar P**, **Pavithra SR**, **Reddy R**, **Venketesh S**, **Kumar R**, **Gupta AK**, **Singh RK**, **Yadav SC**, **Tatu U**. 2010. Heat Shock Protein 90 as a Drug Target against Protozoan Infections: biochemical characterization of HSP90 from *Plasmodium* falciparum and *Trypanosoma* evansi and evaluation of its inhibitor as a candidate drug. J Biol Chem **285**:37964–37975.

33. **Kunzelmann S**, **Webb MR**. 2010. A fluorescent, reagentless biosensor for ADP based on tetramethylrhodamine-labeled ParM. ACS Chem Biol **5**:415–425.

34. **Deng W**, **Parbhu-Patel A**, **Meyer DJ**, **Baker DA**. 2003. The role of two novel regulatory sites in the activation of the cGMP-dependent protein kinase from *Plasmodium falciparum*. Biochem J **374**:559–565.

35. **Bikadi Z**, **Hazai E**. 2009. Application of the PM6 semi-empirical method to modeling proteins enhances docking accuracy of AutoDock. J Cheminform **1**:15.

636 36. **Corbett KD**, **Berger JM**. 2010. Structure of the ATP-binding domain of *Plasmodium*
637 *falciparum* Hsp90. Proteins **78**:2738–2744.

638 37. **Morris GM**, **Goodsell DS**, **Halliday RS**, **Huey R**, **Hart WE**, **Belew RK**, **Olson AJ**. 1998.
639 Automated docking using a Lamarckian genetic algorithm and an empirical binding free
640 energy function. J. Comput. Chem. **19**:1639–1662.

641 38. **Halgren TA**. 1998. Merck molecular force field. I. Basis, form, scope, parameterization,
642 and performance of MMFF94. J. Comput. Chem. **17**:490–519.

643 39. **Solis FJ**, **Wets RJB**. 1981. Minimization by Random Search Techniques. Mathematics of
644 Operations Research **6**:19–30.

645 40. **Taylor HM**, **McRobert L**, **Grainger M**, **Sicard A**, **Dluzewski AR**, **Hopp CS**, **Holder**
646 **AA**, **Baker DA**. 2010. The malaria parasite cyclic GMP-dependent protein kinase plays a
647 central role in blood-stage schizogony. Eukaryotic Cell **9**:37–45.

648 41. **Bozdech Z**, **Llinas M**, **Pulliam BL**, **Wong E**, **Zhu J**, **DeRisi J**. 2003. The Transcriptome
649 of the Intraerythrocytic Developmental Cycle of *Plasmodium falciparum*. PLoS Biol
650 **1**:085–100.

651 42. **Le Roch KG**, **Johnson JR**, **Florens L**, **Zhou Y**, **Santrosyan A**, **Grainger M**, **Yan SF**,
652 **Williamson KC**, **Holder AA**, **Carucci DJ**, **Yates JR**, **Winzeler EA**. 2004. Global
653 analysis of transcript and protein levels across the *Plasmodium falciparum* life cycle.
654 Genome Res **14**:2308–2318.

655 43. **Le Roch KG**, **Zhou Y**, **Blair PL**, **Grainger M**, **Moch JK**, **Haynes JD**, **La Vega De P**,
656 **Holder AA**, **Batalov S**, **Carucci DJ**, **Winzeler EA**. 2003. Discovery of gene function by
657 expression profiling of the malaria parasite life cycle. Science **301**:1503–1508.

658 44. **Liu R**, **Perez-Aguilar JM**, **Liang D**, **Saven JG**. 2012. Binding site and affinity prediction

of general anesthetics to protein targets using docking. Anesth. Analg. **114**:947–955.

45. **Schulte TW**, **Neckers LM**. 1998. The benzoquinone ansamycin 17-allylamino-17-demethoxygeldanamycin binds to HSP90 and shares important biologic activities with geldanamycin. Cancer Chemother. Pharmacol. **42**:273–279.

46. **Bishop AC**, **Kung C-Y**, **Shah K**, **Witucki L**, **Shokat KM**, **Liu Y**. 1999. Generation of Monospecific Nanomolar Tyrosine Kinase Inhibitors via a Chemical Genetic Approach. J Am Chem Soc **121**:627–631.

47. **Bishop AC**, **Ubersax JA**, **Petsch DT**, **Matheos DP**, **Gray NS**, **Blethrow J**, **Shimizu E**, **Tsien JZ**, **Schultz PG**, **Rose MD**, **Wood JL**, **Morgan DO**, **Shokat KM**. 2000. A chemical switch for inhibitor-sensitive alleles of any protein kinase. Nature **407**:395–401.

48. **Larochelle S**, **Merrick KA**, **Terret M-E**, **Wohlbold L**, **Barboza NM**, **Zhang C**, **Shokat KM**, **Jallepalli PV**, **Fisher RP**. 2007. Requirements for Cdk7 in the assembly of Cdk1/cyclin B and activation of Cdk2 revealed by chemical genetics in human cells. Mol Cell **25**:839–850.

49. **Endo S**, **Satoh Y**, **Shah K**, **Takishima K**. 2006. A single amino-acid change in ERK1/2 makes the enzyme susceptible to PP1 derivatives. Biochem Biophys Res Commun **341**:261–265.

50. **Weiss EL**, **Bishop AC**, **Shokat KM**, **Drubin DG**. 2000. Chemical genetic analysis of the budding-yeast p21-activated kinase Cla4p. Nat Cell Biol **2**:677–685.

51. **Stebbins CE**, **Russo AA**, **Schneider C**, **Rosen N**, **Hartl FU**, **Pavletich NP**. 1997. Crystal structure of an Hsp90-geldanamycin complex: targeting of a protein chaperone by an antitumor agent. Cell **89**:239–250.

52. **Banumathy G**, **Singh V**, **Pavithra SR**, **Tatu U**. 2003. Heat shock protein 90 function is

essential for *Plasmodium falciparum* growth in human erythrocytes. J Biol Chem **278**:18336–18345.

53. **Shahinas D**, **Folefoc A**, **Taldone T**, **Chiosis G**, **Crandall I**, **Pillai DR**. 2013. A purine analog synergizes with chloroquine (CQ) by targeting *Plasmodium falciparum* Hsp90 (PfHsp90). PLoS ONE **8**:e75446.

54. **Wang T**, **Bisson WH**, **Mäser P**, **Scapozza L**, **Picard D**. 2014. Differences in Conformational Dynamics between *Plasmodium falciparum* and Human Hsp90 Orthologues Enable the Structure-Based Discovery of Pathogen-Selective Inhibitors. J Med Chem **57**:2524–2535.

55. **Lourido S**, **Tang K**, **Sibley LD**. 2012. Distinct signalling pathways control *Toxoplasma* egress and host-cell invasion. EMBO J **31**:4524–4534.

56. **Glushakova S**, **Lizunov V**, **Blank PS**, **Melikov K**, **Humphrey G**, **Zimmerberg J**. 2013. Cytoplasmic free Ca2+ is essential for multiple steps in malaria parasite egress from infected erythrocytes. Malaria Journal **12**:41.

57. **Dvorin JD**, **Martyn DC**, **Patel SD**, **Grimley JS**, **Collins CR**, **Hopp CS**, **Bright AT**, **Westenberger S**, **Winzeler E**, **Blackman MJ**, **Baker DA**, **Wandless TJ**, **Duraisingh MT**. 2010. A plant-like kinase in *Plasmodium falciparum* regulates parasite egress from erythrocytes. Science **328**:910–912.

58. **Sams-Dodd F**. 2005. Target-based drug discovery: is something wrong? Drug Discov. Today **10**:139–147.

Table 1. Compounds divided into two classes based on the aromatic linker, class 1 (pyrimidine) and class 2 (non-pyrimidine). EC_{50} values of compounds were determined using the SYBR Green I assay following treatment of parasite cultures with serial dilutions of the compounds for 48 h or 96 h. Data presented show the mean EC_{50} from three independent experiments, with the standard deviation shown in parentheses. The stage of action was determined by microscopic examination of Giemsa-stained parasite smears after treatment of ring stage parasites with 10-times the 96 h EC_{50} concentration of compound for 48 h.

Compound	Aromatic linker	EC_{50}, µM (SD)		EC_{50}48/EC_{50}96 ratio	Stage of action by microscopy
		48h	96h		
Class 1					
28	pyrimidine	0.168 (0.011)	0.038 (0.012)	4.4	late schizont
31	pyrimidine	1.663 (0.650)	0.238 (0.047)	7.0	late schizont
35	pyrimidine	> 1000	0.809 (0.451)	> 1000	late schizont
36 (Cpd A)	pyrimidine	> 1000	0.023 (0.007)	> 1000	late schizont
38	pyrimidine	> 1000	0.050 (0.018)	> 1000	late schizont
39 (Cpd B)	pyrimidine	> 1000	0.020 (0.008)	> 1000	late schizont
41 (Cpd C)	pyrimidine	> 1000	0.037 (0.005)	> 1000	late schizont
Class 2					
7 (Cpd D)	pyridine	0.355 (0.083)	0.311 (0.103)	1.1	trophozoite
20 (Cpd E)	fluoropyridine	0.298 (0.066)	0.142 (0.024)	2.1	trophozoite
22	pyridine	0.546 (0.080)	0.300 (0.141)	1.8	trophozoite

712 **Table 2. Class 1 compounds inhibit PKG and their potency against both the enzyme and the parasite is reduced by a larger**
713 **gatekeeper residue.** Class 1 pyrimidine-linked compounds in particular display potent inhibition of PKG but not the T618Q variant.
714 Parasite inhibition data are calculated from a single experiment, other than duplicate assays performed on compounds A, C, and D. For
715 these compounds the mean EC_{50} is shown, with the standard deviation from the mean in parentheses.
716

Compound	Aromatic linker	Enzyme inhibition IC_{50} (μM)			Selectivity	Parasite inhibition EC_{50} (μM)		EC_{50} ratio
		CDPK1	PKG	PKG T618Q	PKG T618Q/ PKG	3D7	3D7 PKG T618Q	3D7 PKG T618Q/ 3D7
Class 1								
28	Pyrimidine	0.012	0.003	31.69	12100	0.059	0.640	11
36 (Cpd A)	Pyrimidine	0.008	0.002	10.96	5641	0.034 (0.006)	0.901 (0.483)	27
38	Pyrimidine	0.008	0.004	43.52	12187	0.073	0.859	12
39 (Cpd B)	Pyrimidine	0.009	0.002	25.54	16520	0.034	0.982	29
41 (Cpd C)	Pyrimidine	0.011	0.013	12.70	957	0.042 (0.018)	0.923 (0.226)	22
44	Pyrimidine	0.065	nd	nd	—	0.236	0.477	2
Class 2								
7 (Cpd D)	Pyridine	0.013	0.484	15.51	32	0.427 (0.045)	0.477 (0.180)	1
20 (Cpd E)	Fluoropyridine	0.008	0.012	15.33	1325	0.210	0.386	2
22	Pyridine	0.074	>1	37.53	<38	0.215	0.303	1
42	Pyridine	0.081	nd	nd	—	0.836	1.231	1
43	Pyridine	0.088	nd	nd	—	0.080	0.093	1
Cpd 1						0.303	1.974	7

717
718

Figure legends

Figure 1. Imidazopyridazine compounds have two modes of action.

A. Imidazopyridazine compounds in this study are characterised by an invariant core, an aromatic linker group (A) and variable R1 and R2 groups. **B.** *P. falciparum* 3D7 parasites approximately 21 hours after merozoite invasion of erythrocytes were incubated for 48 h with a concentration equal to 10-times the EC_{50} of each compound (determined by FACS (23)). In mock-treated cultures (0.05 % DMSO) newly invaded erythrocytes with ring-stage parasites are seen. In the presence of compound C (0.3 µM) parasites developed until very late schizogony, then arrested prior to merozoite egress, whereas with compound D (4 µM), parasites failed to develop beyond late rings/early trophozoites. **C.** EC_{50} determination using a SYBR Green I assay. *P. falciparum* cultures were incubated for either 48 h or 96 h with serial dilutions of inhibitors. For compound A, the EC_{50} with 48 h incubation was not able to be determined with any accuracy, whereas with 96 h incubation the EC_{50} was 0.023 µM (SD = 0.007). The EC_{50} for compound E was 0.298 µM (SD = 0.066) or 0.142 µM (SD = 0.024) with 48 h or 96 h incubation respectively. The graphs shown are representative examples of triplicate experiments. Error bars show the standard error of the mean for duplicate samples.

Figure 2. Parasite killing activity of class 1 compounds can be attributed to inhibition of cGMP-dependent protein kinase.

A.(i) Correlation between *P. falciparum* EC_{50} and PKG IC_{50} for 13 class 1 compounds. The calculated coefficient of determination (r^2) value of 0.71 from a linear least squares

regression indicates a good correlation between the two data sets. A p value of 0.0002 signifies indicates a significant relationship between the two measurements. **(ii)** Correlation between *P. falciparum* EC_{50} and PKG IC_{50} for 16 class 2 compounds. r^2 = 0.17 indicates little correlation between the 3D7 EC_{50} and the PKG IC_{50} for class 2 compounds. In addition, a p value of 0.114 indicates that there is no significant relationship between the two measures. **B.** Parasites expressing a large gatekeeper variant PKG (3D7 PKG T618Q) are insensitive to compound C compared to WT parasites (3D7 PKG WT). SYBR Green assays were used to measure the parasitemia of cultures treated with serial dilutions of compound C for 96 h. The experiment was performed twice; data from a single experiment are shown. The EC_{50} values are 0.923 µM (SD = 0.226) for 3D7 PKG T618Q and 0.042 µM (SD = 0.018) for 3D7 PKG WT parasites. Error bars represent the standard error of the mean of duplicate samples. **C.** Mann-Whitney test to compare the ratio of EC_{50} values for 3D7 PKG T618Q:3D7 WT PKG treated with class 1 and class 2 compounds. Horizontal bars show the median value for each class of compounds (16.8 for class 1, 1.4 for class 2). The calculated p value is 0.0043.

Figure 3. Affinity purification of cellular targets of compound D.

A. Biotin linked to the R1 group of compound D. This compound was bound to streptavidin-agarose and used to affinity purify proteins from a trophozoite cell lysate. The only significant hit identified by LC-MS/MS was HSP90 (Table S3). **B.** Predicted interactions between compound D and PfHSP90. **C.** Modelling of the most likely binding orientation of compound D to the ATP-binding site of HSP90 was carried out using DockingServer. Residues predicted to form hydrogen bonds with compound D are

765 labelled in green, while those predicted to form hydrophobic interactions are labelled in
766 blue. **D.** Recombinant PfHSP90 binds to compound D. Purified recombinant PfHSP90
767 and PfHSP90-NTD used in subsequent experiments are shown in the Coomassie stained
768 gels to the left of the figure. Changes in the tryptophan fluorescence (346 nm) of
769 PfHSP90 were monitored in the presence of increasing amounts of compound D or 17-
770 AAG. K_d values were calculated for both full length (FL) PfHSP90 and PfHSP90-NTD.
771 Values in brackets are the standard error of the mean of triplicate measurements.
772
773 **Figure 4. Inhibition of PfCDPK1 has no effect on asexual parasite growth.**
774 **A.** Chemical structures of the bumped kinase inhibitors (BKIs) NA-PP1 and NM-PP1. **B.**
775 Recombinant CDPK1 with a glycine at the gatekeeper residue (amino acid 145) shows
776 increased sensitivity to both BKIs. A ParM ADP biosensor assay to measure ATPase
777 activity of CDPK1 enzymes was carried out in the presence of serial dilutions of BKIs.
778 The IC_{50} of CDPK1 T145G for NA-PP1 decreased 41-fold compared to WT CDPK1,
779 with IC_{50} values of 0.15 µM [95% confidence intervals (CI) 0.08 to 0.26 µM] and 6.01
780 µM [95% CI 3.4 to 10.5 µM] respectively. The IC_{50} of NM-PP1 was 0.12 µM [95% CI
781 0.06 to 0.23 µM] for CDPK1 T145G compared to 1.5 µM [95% CI 0.77 to 2.90 µM] for
782 WT CDPK1, a 13-fold decrease. Graphs show mean values from five independent
783 experiments, with error bars indicating the standard error of the mean. **C.** Scheme for
784 generating a *P. falciparum* 3D7 CDPK1 T145G-HA parasite line by single crossover
785 homologous recombination at the *cdpk1* genomic locus. Crossover upstream of the T145
786 codon is forced by recodonising sequences downstream of and including the T145 codon.
787 Integration at the locus results in a chimeric *cdpk1* gene with a modified gatekeeper

residue. An identical method was used in which the gatekeeper residue was left as a threonine to generate the parasite line 3D7 CDPK1 T145T-HA. **D.(i)** Whole cell lysates from *P. falciparum* 3D7, 3D7 CDPK1 T145T-HA (T) and 3D7 CDPK1 T145G-HA (G) were probed with antibodies against CDPK1 (left panel), and against the HA epitope tag (right panel). **(ii)** Immunofluorescence using anti-HA and anti-CDPK1 antibodies confirms that CDPK1 T145G-HA localizes correctly to the plasma membrane of parasites. Scale bar is 1 µm. **E.** SYBR Green assays to measure EC_{50} values of *P. falciparum* 3D7 CDPK1 T145T-HA and 3D7 CDPK1 T145G-HA lines to NA-PP1 and NM-PP1. The EC_{50} for NA-PP1 in 3D7 CDPK1 T145T-HA was 14.26 µM [95% CI 12.3 to 16.5] and in 3D7 CDPK1 T145G-HA was 15.65 µM [95% CI 13.4 to 18.3]. The EC_{50} for NM-PP1 was 11.55 µM [95% CI 9.1 to 14.6] and 10.28 µM [95% CI 8.1 to 13.0] for 3D7 CDPK1 T145T-HA and 3D7 CDPK1 T145G-HA respectively. The experiments were performed three times, with at least six replicate samples per experiment. Graphs show mean values from three independent experiments, with error bars indicating the standard error of the mean.

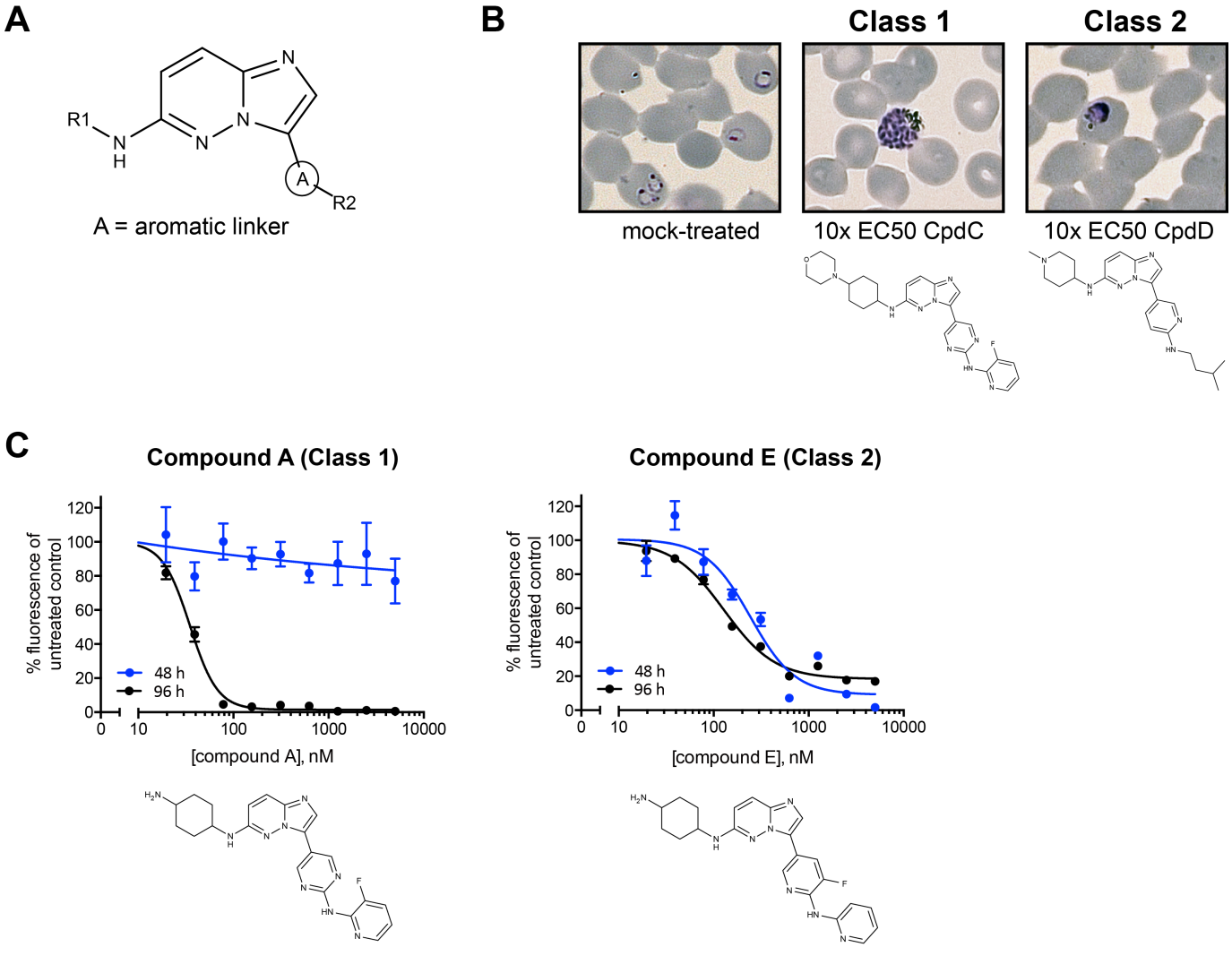

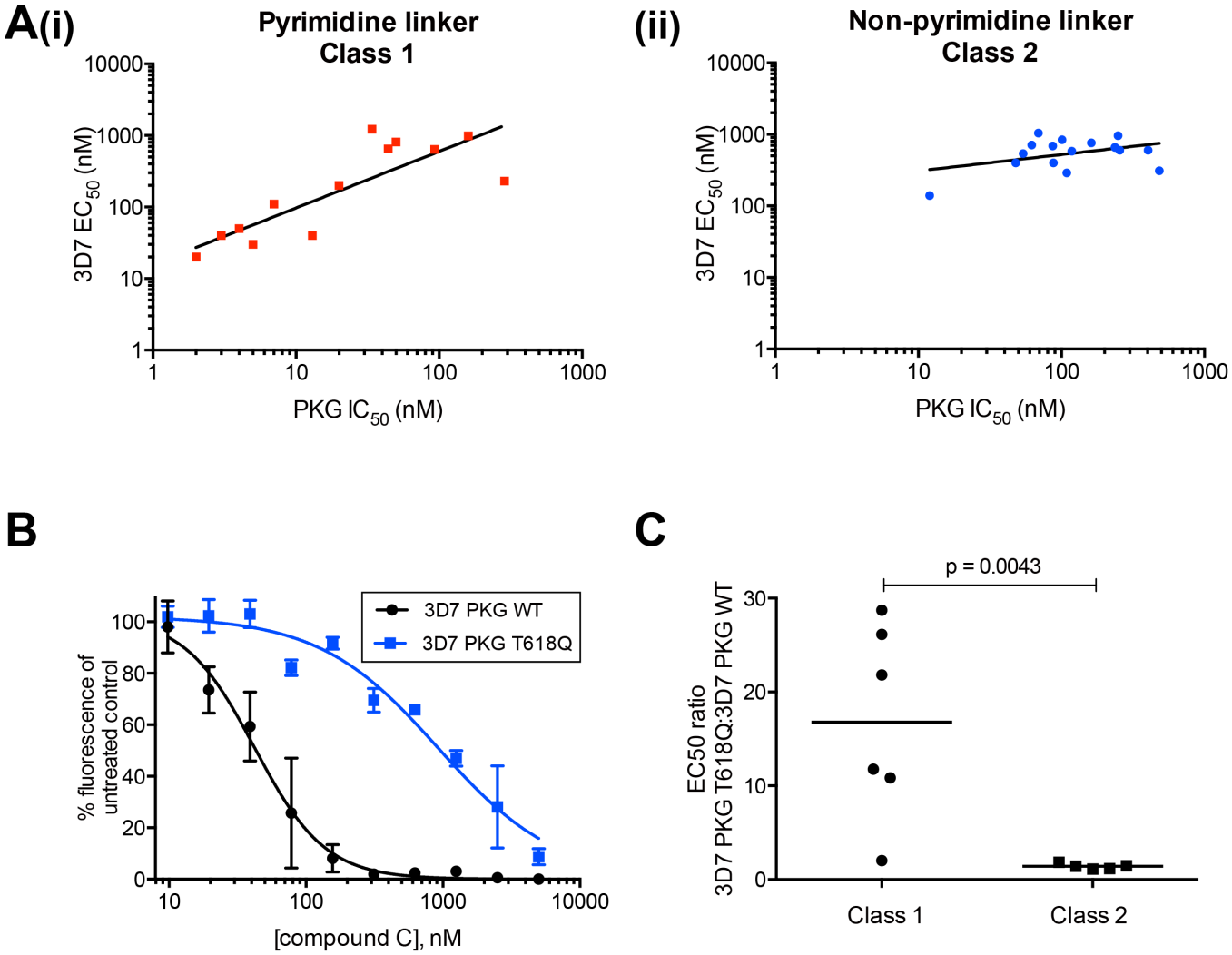

A

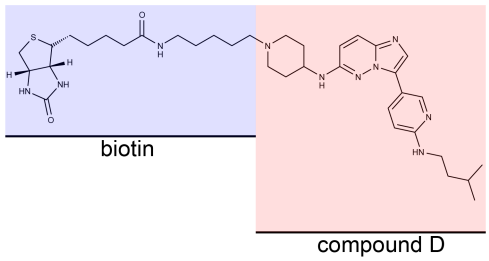

B

Predicted interactions between compound D and PfHSP90 (kcal/mol)

Hydrogen bonds	Hydrophobic
ASN37 (-1.8386)	PHE124 (-1.4225)
ASP40 (-0.3766)	LEU34 (-0.5926)
	LEU93 (-0.5256)
	ALA38 (-0.4258)
	ILE173 (-0.406)

C

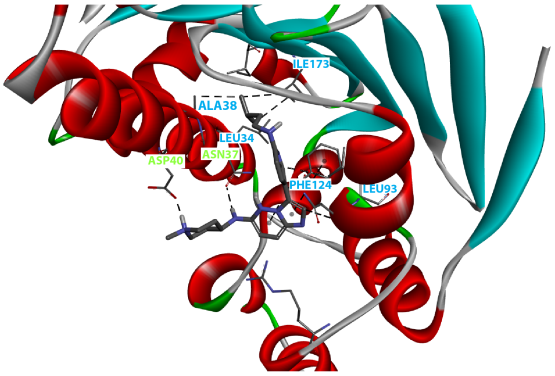

D

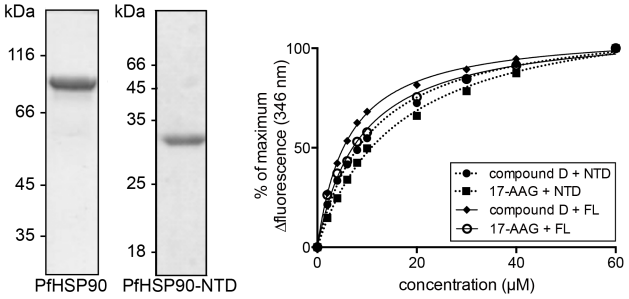

	Kd (μM) [SE]	
	compound D	17-AAG
PfHSP90-NTD	10.73 [0.62]	15.84 [0.93]
PfHSP90	6.17 [0.18]	8.70 [0.69]